Journal of Materials Chemistry A

Accepted Manuscript

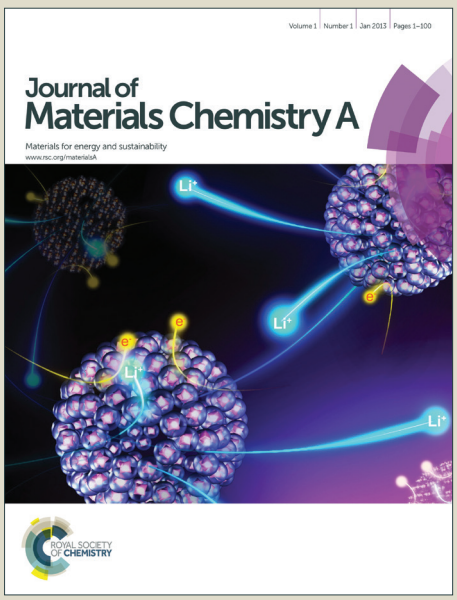

ROYAL SOCIETY OF CHEMISTRY

www.rsc.org/materialsA

Journal of Materials Chemistry A

Journal of Materials Chemistry A

Dynamic Article Links ►

Cite this: DOI: 10.1039/c0xx00000x

ARTICLE TYPE

www.rsc.org/xxxxxx

Mechanically bendable superhydrophobic steel surface with its self-cleaning and corrosion-resistant properties

Sanjay S. Latthe [a], P. Sudhagar [a], Anitha Devadoss [a], A. Madhan Kumar [b], Shanhu Liu [c], Chiaki Terashima [a], Kazuya Nakata [a], and Akira Fujishima* [a]

Received (in XXX, XXX) Xth XXXXXXXXX 20XX, Accepted Xth XXXXXXXXX 20XX
DOI: 10.1039/b000000x

We present an effective way to develop superhydrophobic steel surface which shows stable superhydrophobicity under harsh mechanical bending. The roughness on steel surface was created by etching in acid solution and its surface energy was lowered by subsequent hydrophobic silane treatment. The steel etching time in sulfuric acid solution was optimized to 8 h which provides high surface roughness required for superhydrophobicity. A water contact angle of 164±3º and sliding angle of 9±2º was obtained on the steel surface after surface chemical modification by methyltrichlorosilane. We bent this superhydrophobic steel to 90º and 180º and studied wetting properties on bent area, which showed absolute no change in superhydrophobicity. This superhydrophobic steel surface showed excellent self-cleaning behaviour as well as maintained its superhydrophobic wetting properties under stream of water jet. Further the stability of the wetting state was evaluated using sandpaper abrasion test, adhesive tape peeling test, and under prolonged UV irradiation. The energy-dispersive X-ray spectroscopy was used to confirm the surface chemical composition of the superhydrophobic steel surface. This approach can be used to apply on steel surface of any size and shape to advance their industrial applications.

Introduction

Nature is a *'Top University'* in the world and scientists from diverse scientific field learn there for free. One of the fascinating branches of nature is the branch of extremely non-wettable surfaces. On the natural non-wettable surfaces, liquid drops achieve sphere shape and immediately roll off the surface due to extremely low adhesion. While rolling off, the liquid drop eventually carry away any dust particles existing on the surface, performing self-cleaning behaviour. The extreme water repellent and self-cleaning surfaces, on which a water drop acquires contact angle greater than 150º and roll off quickly at minute disturbance, are famously known as superhydrophobic surfaces. In nature, especially the lotus leaves [1], wings of butterflies [2] and legs of water strider [3] are known for their extreme water repellency and self-cleaning properties. The scientific reason behind the superhydrophobicity of these naturally occurring surfaces are most studied, widely researched and well discussed in the literature. The surface roughness plays an important role in determining the wetting state of solid surface. The two wetting states on rough solid surfaces are famously known as Wenzel's [4] and Cassie-Baxter's [5] wetting states. In the Wenzel's state [4], the liquid drop could easily penetrate and wet the rough structure resulting high adhesion towards the surface. However, in the Cassie-Baxter's state [5], liquid does not penetrate due to the trapped air pockets in between the rough structure, and the liquid drop sits on the top asperities of the structure maintaining high contact angle and roll off at small tilt angles. A dual scaled rough structure in conjunction with low surface energy is prerequisite to achieve superhydrophobic surfaces [6]. Highly inspired by the natural superhydrophobic surfaces, tremendous research has been carried out since past two decades to develop artificial superhydrophobic coatings on glass [7-9], plastics [10], mesh [11], papers [12, 13], fabrics [14, 15] metals [16, 17], and others [18] for self-cleaning, anti-icing, drag reduction, oil-water separation and anti-corrosive applications. Today superhydrophobic research field is expanding enormously due to its outstanding industrial applications.

Superhydrophobic metal surfaces can be easily achieved by simple acid and/or base treatments and subsequent surface chemical modification [19]. The etching of metals in acid or base solutions can simply create dual scale rough structure required to achieve superhydrophobicity after surface chemical modification by low surface energy materials. This strategy has been broadly used to achieve superhydrophobicity on metal substrates like steel [20], copper [21], aluminium [22] and zinc [23]. The large numbers of high energy dislocation sites present in crystalline metals are prone to destroy when immersed in chemical etchants leading to the formation of micron scale surface roughness. Qian and Shen [23]

reported a simple dislocation selective chemical etching process to achieve superhydrophobicity on polycrystalline aluminum, copper, and zinc substrates after subsequent fluoroalkylsilane surface modification. The dislocation etchant can preferentially dissolves the dislocation sites in the grains, creating highly rough surface. Recently, Li et al [24] adopted a simple three step solution immersion method; etching in hydrochloric acid solution, hot water treatment and surface chemical modification by stearic acid to obtain lotus leaf like surface morphology on aluminium foil which exhibited excellent superhydrophobicity. This superhydrophobic aluminium foil provided good friction-reduction ability, excellent self-cleaning performance and stable superhydrophobicity even after immersion in 3.5 wt. % NaCl aqueous solution for more than 2 days. Liu et al. [25] prepared a superhydrophobic Cu surface with dual-scale convex polyhedral protrusions with regular shapes by selective etching of high-energy facets in H_2O_2/HCl etchant solution and subsequent stearic acid surface modification. This superhydrophobic Cu surface showed stable superhydrophobicity with a water contact angle of 165°, even after ultrasonicated for 1 h. After immersing the sample in aqueous solutions with various pH values for 3 days, the superhydrophobic Cu surface exhibited a contact angle of more than 158° for all pH solutions. During the abrasion test, a normal pressure (~5 kPa) was applied to the superhydrophobic Cu surface and slided on a common cotton fabric in one direction for a distance of 25 cm. The water contact angle of superhydrophobic Cu surface decreased to 153° due to partial loss of the surface roughness and stearic acid molecules during abrasion test. In the present research work, we optimized the etching time in sulfuric acid solution to get rough surface on steel and achieved superhydrophobicity after surface chemical modification by methyltrichlorosilane. This superhydrophobic steel surface showed excellent self-cleaning behaviour as well as maintained its superhydrophobic wetting state under stream of water jet and harsh mechanical bending. Compared to previous reports on flexible superhydrophobic surface,[26-28] this work doesn't require tedious experimental procedure. A rough and porous organosilica layer was found intact without damage under harsh mechanical bending confirming its flexibility.

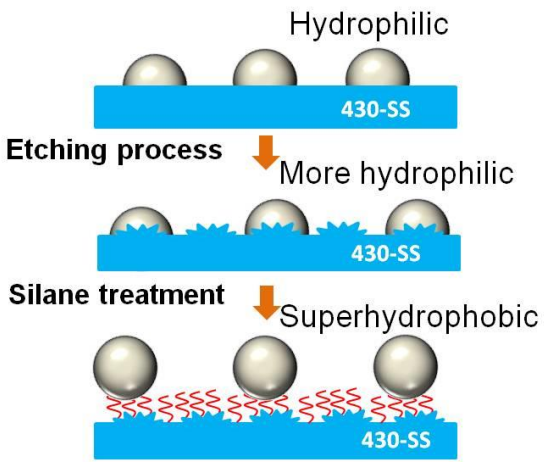

Scheme 1. Illustration of experimental protocol for fabricating superhydrophobic steel surface.

Experimental

Materials

Stainless steel 430 (SS) were used as substrates, obtained from The Nilaco Corporation, Tokyo Ginza, Japan. Sulfuric acid (2N), ethanol (99.9%), and Oil Red O (154-02072) were purchased from Wako Pure Chemical Industries Ltd, Japan. Methylene Blue (M0501) was bought from Tokyo Kasei Kogyo Co. Ltd, Japan. Methyltrichlorosilane (MTCS, ≥97%), was purchased from Sigma Aldrich, USA.

Preparation of superhydrophobic stainless steel surfaces

At first, the stainless steel substrates were ultrasonically cleaned with double distilled water and ethanol for 30 min and dried at room temperature. As shown in scheme 1, the cleaned stainless steel substrates were immersed in sulphuric acid solution for etching. The etching process starts after 3 h of immersion time, so the etching time reported here are those recorded after 3 h. The etching time was varied from 1 to 12 h to achieve optimum surface roughness required for superhydrophobicity. After taking out from sulphuric acid solution, the substrates were ultrasonically cleaned with double distilled water for 30 min and then dried at room temperature. These etched substrates were immersed in fresh 10 vol. % MTCS in hexane for 2 h for surface chemical modification and finally annealed at 200 ºC for 2 h. For ease in discussion, the bare, etched and chemically modified stainless steel substrates were named as B-430-SS, E-430-SS, and M-430-SS, respectively.

In the present investigation, we have performed the chemical modification in two stages. At first, the SS surface was chemically etched using sulphuric acid. In general, 430 SS grade substrates are passive when exposed to sulphuric acid due to oxide film formed on the SS surface. Based on chemical composition of 430 SS substrate, the passive layer contains the metal oxides namely Cr_2O_3, Fe_2O_3 and Mn_2O_3 in the substrate; among these oxide layers Cr_2O_3 is present in the inner layer. The purpose of a passivation is to strengthen the natural protective oxide film of the steel, and in addition, non-metallic inclusions as well as high energy dislocation sites are largely dissolved during acid treatment forming a rough surface associated with existence of hydroxyl groups on the etched steel surface. In the second step, the acid etched SS substrates were modified with chemical treatment using MTCS. The SS substrate is immersed in MTCS solution for 2h. As the MTCS contains 3 functional groups, they undergo hydrolysis and condensation reactions in the presence of hydroxyl groups and finally form thin organosilica layer on the SS surface [29].

Characterization

The surface morphology of the substrate was studied by Field Emission Scanning Electron Microscope (JEOL, JSM-7600F). The surface chemical analysis of the substrate was made by energy dispersive x-ray spectroscopy (EDX) (JEOL, EX-64235 ACSW) using the substrate area of ~ 100 μm^2. Laser microscope (KEYENCE, VK-X200 series) was used to analyse the surface topography and roughness of the substrates. The surface roughness was measured in 50×50 μm^2 planar in non-contact mode. The surface roughness of each samples were measured for at least six different positions and average was reported as a final value. The water contact angles on each sample were measured

for at least six different places and average value was adopted using contact angle meter (KYOWA, model DM-301). The angle at which the water drop deliberately slides off the surface is reported as sliding angle. An abrasion test was performed by placing the superhydrophobic steel surface facing towards the sandpaper (600 grit silicon carbide sandpaper, Bellstar Abrasive Mfg., Japan) and a weight of 500 g was placed on the top of it. Then the sample was subject to unidirectional drift with speed of 10 mm/s for the distance of ~100 cm. Further, an adhesive tape peeling test was accomplished by using two sided adhesive tape (NW-H25, Nichiban Co. Ltd., Japan). The adhesive tape was placed and pressed gently on the superhydrophobic steel surface to achieve uniform contact between the tape and surface. The adhesive tape was then slowly removed to study the surface properties. The wetting properties, FE-SEM and laser microscope images of the surface, before and after the sandpaper abrasion and adhesive tape peeling test were studied. The effect of UV irradiation time on the wetting properties of superhydrophobic steel surface was studied by using UV light source (365 nm, 2 mW/cm^2, Toshiba Carporation, Japan).

Results and discussions

Surface morphology and topography

The surface morphology plays an important role in the development of superhydrophobic surfaces. **Fig. S1** shows the typical surface morphology of the bare SS and SS substrates etched for different time intervals. The bare stainless steel surface shows smooth morphology, whereas the substrate eventually gets rough with etching time. After 1 h of etching, smooth morphology of the bare stainless steel changed to rough morphology, but the extent of rough structure is not uniform all over the surface. The rough structure was not uniform until the 6 h of etching time. However, as shown in **Fig. 1a**, after 8 h of etching time, the SS substrate showed uniform rough structure. In higher magnification (**Fig. 1b)** it shows domain-like rough microstructure with presence of many voids. This rough surface was thinly and uniformly covered by porous organosilica layer originated from MTCS modification (**Fig. 1c**). This modified surface morphology extensively resembles lotus leaf surface, where the rough microscale papillae structure is covered by nanoscale wax material [1].

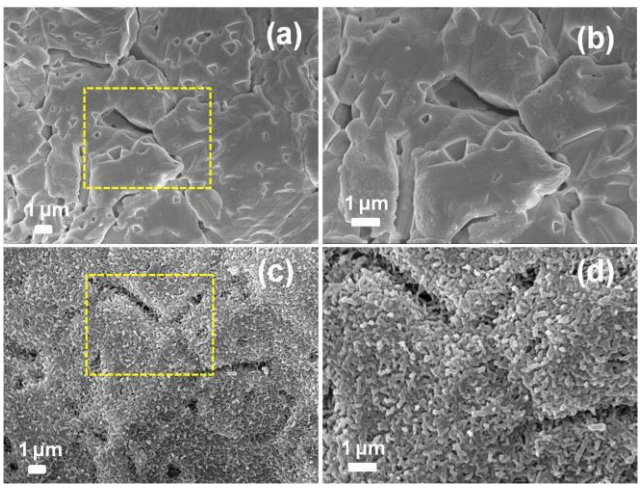

Figure 1. FE-SEM images of (a) E-430-SS/8h and (b) high magnification image of marked portion at Fig.1(a); (c) M-430-SS/8h and (d) high magnification image of marked portion at Fig.1(c).

The laser microscope images of bare, etched and modified SS surface are shown in **Fig. 2**. A smooth bare SS substrate showed the surface roughness of 0.28 µm. The surface roughness was remarkably increased to 7.97 µm after etching, whereas after MTCS modification, the surface roughness was decreased to 2.33 µm. The extensive gaps and voids present on the etched steel surface was uniformly filled and thinly covered by organosilica layer which results in decrease in surface roughness.

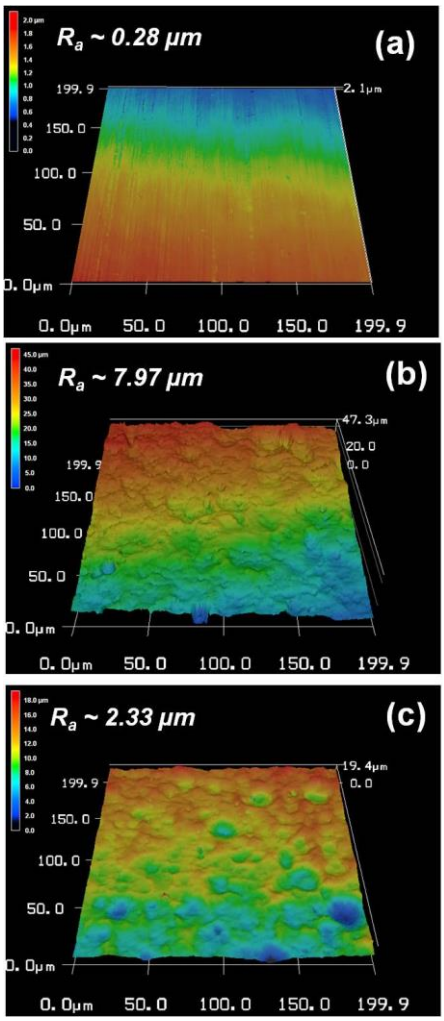

Figure 2. Laser microscope images of (a) B-430-SS (b) E-430-SS/8h (c) M-430-SS/8h.

The EDX spectrum of the bare stainless steel exhibits carbon (C), oxygen (O), iron (Fe), aluminium (Al), chromium (Cr) and manganese (Mn) peaks because the stainless steel is usually made up from all these chemical elements (**See Supporting information Fig. S2a**). The surface modified stainless steel surface shows the peaks of only C, O and silica (Si) confirming the coverage of steel surface by hydrophobic Si-O-CH_3 groups from MTCS (**See Supporting information Fig. S2b**).

Wetting property of the coating

The water contact angle measurement is one of the important major to study the wettability of the solid surfaces. The wettability of the steel surfaces etched for different etching time was studied after subsequent surface modification. The water drop of ~ 8 µl was used during the contact angle measurements.

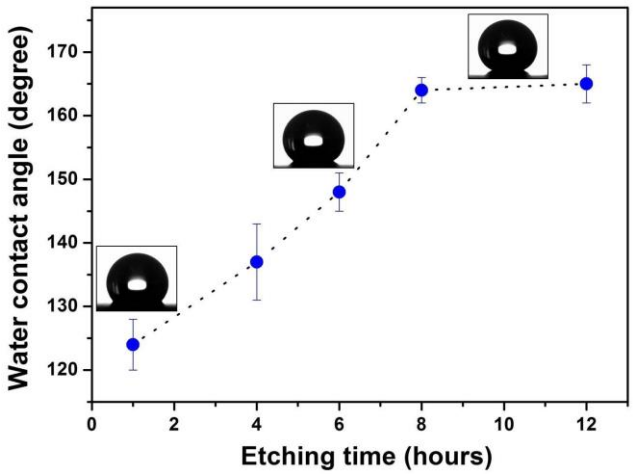

Figure 3. Water contact angles on steel surface etched for different etching time.

As shown in **Fig. 3**, the steel surface etched for 1 h revealed the water contact angle of 124º. Even though, the surface is in hydrophobic state, the water drop could not slide off the surface and the drop sticks to the surface even after tilting the surface for 90º or tilted upside down. This shows the strong adhesion between the water drop and surface. The water drop could be off the surface only after strong jerk given to the substrate, but still some water impression remained on the surface. This can be called as a sticky hydrophobicity. This same trend of wetting state was observed for the surface etched for 4 and 6 h. For 4 and 6 h etching, the steel surface showed the water contact angle of 137º and 148º, respectively, and these surfaces showed strong adhesion towards water drop similar to the 1 h etched steel surface. After bringing the water drop (~ 4µl) hanged on needle towards the surfaces etched for 1 to 6 h, the water drop immediately lands on surface. This wetting state can be ascribed to Wenzel's wetting state, where the water drop could easily penetrate the non-homogeneous rough structure and stay pinned to the surface. However, the Wenzel state wetting switched to Cassie-Baxter state after 8 h etching time. The water drops achieve a contact angle of 164º and roll off the surface at tilt angle of only 9º, performing in highly superhydrophobic state. After bringing the water drop (~ 4µl) hanged on needle towards this surface, the water drop could not land on the surface and keep hanging on the needle due to extreme non-wettability of the surface. In this case, the water drop volume was increased to 8µl, so that water drop could land on the superhydrophobic surface as the result of gravitational force.

Fig. 4 shows optical photograph of the water drops on bare, etched and modified steel surface. For better optical clarity of the water drops, they were stained blue using methylene blue. **Fig. 4(a)** shows the water drop on bare steel surface which shows the contact angle of 70º, whereas the water drops eventually spreads on 8h etched steel surface making the contact angle of just 43º (**Fig. 4b**). This strong hydrophilic property of 8h etched steel surface get converted to superhydrophobic after MTCS surface modification and all water drops acquire spherical shape along with high contact angle exhibiting the Cassie–Baxter state (**Fig. 4c**). The water drops were not stable on the surface and eventually rolled off the surface under small disturbance. This confirms that the adhesion between the water drop and steel surface is very weak because the area under the water droplet is actually liquid-air interface instead of solid-liquid interface. No significant changes observed in wettability upon further etching time to 12 h.

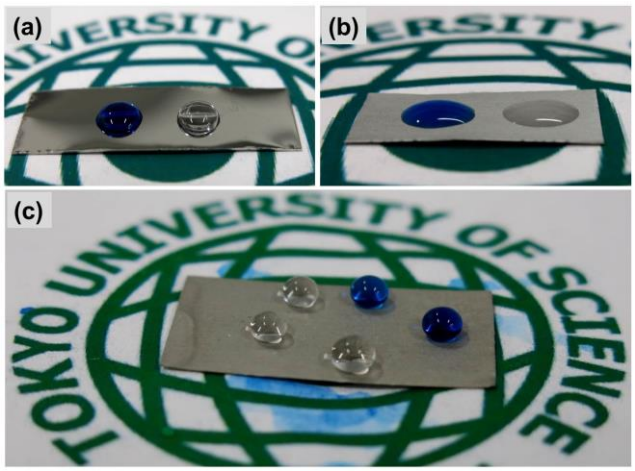

Figure 4. Optical photographs of water drop on (a) B-430-SS (b) E-430-SS/8h (c) M-430-SS/8h.

Wetting Stability of the Surface against Mechanical Bending

The superhydrophobic wetting state of the metal surfaces should get preserved under mechanical bending to expand their industrial applications. We bent the superhydrophobic steel surface up to 90º and more than 90º and studied the wetting state at bent area.

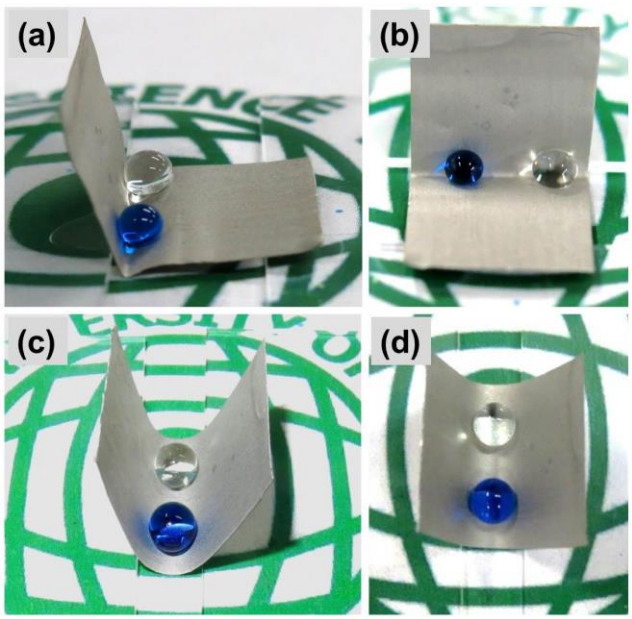

Figure 5. Optical photographs of water drop on bendable (90°) M-430-SS/8h surface at different views (a) cross view, (b) front

view; bendable M-430-SS/8h surface >90° (c) side view and (d) top view.

Fig. 5 shows the different views of the water drops on bent superhydrophobic steel surface. For both the cases, the bent area showed no change in superhydrophobic wetting state. We observed no pinning of the water drops in bent area. The water drops maintained their spherical shape and rolled off immediately by small air blow or under little mechanical disturbance. Guo et al [30] have successfully tested stable wetting properties of superhydrophobic zinc plate covered by copper film after limited bending (<100°). To confirm the durability of the superhydrophobic wetting state under harsh mechanical bending, the superhydrophobic steel surface was completely bent (~180º) in the middle and released to the original position. We could not make the surface perfectly flat and the kink was still maintained in the middle. We placed the water drops on the kink region, where the water drops were still maintained the spherical shape and rolled off easily, confirming no change in wettability under harsh mechanical bending conditions (**Fig. 6b**). We repeated bending the superhydrophobic steel surface for more than 25 times and each wettability test showed no change in superhydrophobic state. A video of water drops bouncing from the bent area is shown in supporting information. **Fig. 6c** depicts the FE-SEM image of bent superhydrophobic steel surface which confirms no substantial change in surface morphology. A few trivial micro-cracks were observed on the bent surface however the porous silica layer was found intact. As a result, the wetting properties of the bent steel surface remain unaltered.

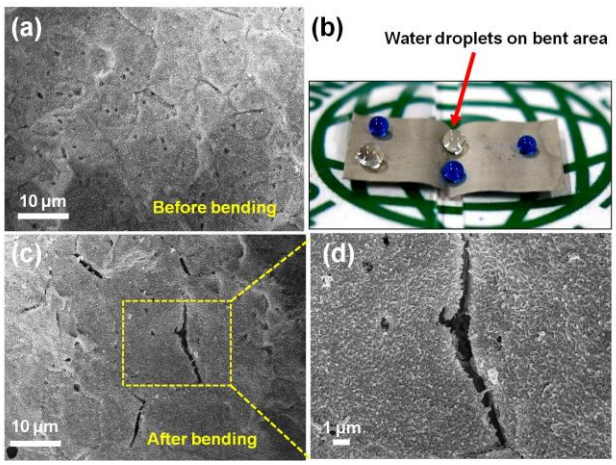

Figure 6. (a) FE-SEM image of M-430-SS/8h before bending, (b) optical photograph of water drops on M-430-SS/8h surface after bending at 180º and released back to original position, (c) FE-SEM image of M-430-SS/8h after bending and (d) high magnification image of marked portion at Fig.6(c).

The flat as well as bent superhydrophobic steel surface showed no change in the wettability even after storage in open environment for more than 12 months. The wetting state of superhydrophobic steel surface was preserved under gentle feather touching by finger tips. We have also checked the stability of the superhydrophobic wetting state under ultrasonic treatment. For continuous 15 min of ultrasonic treatment, the wettability of the superhydrophobic steel surface was not changed substantially and the contact angle measured was around 160º. However, after 30 min of constant ultrasonication, steel surface showed decrease in water contact angle to 103º. The removal of hydrophobic organosilica layer from the surface under ultrasonic treatment is the main reason for loss of superhydrophobicity. However, the superhydrophobicity was regained by MTCS surface modification.

Wetting stability of the surface under perturbation conditions

The development of mechanically stable superhydrophobic surfaces is crucial task as the rough surface structure can prone to destroy by little mechanical brushing. An impacting water stream can irreversibly ruin the extreme water repellent property of the superhydrophobic surface[31-33]. Usually on superhydrophobic surface, water jet perform elastic collision [34]. Any damage to the surface microstructure or surface chemical groups would result the water jet to wet the surface. In the present study, a syringe was filled by the blue coloured water and water jet was produced by syringe pressing rate of ~ 2mm/s (needle diameter~0.8mm). As shown in **Fig. 7**, water jet hit the bare steel surface (**Fig. 7 a**) and 8 h etched steel surface (**Fig. 7 b**) and spreads immediately without bouncing off. This is particularly due to the smooth surface of bare steel surface and hydrophilic nature of the 8 h etched rough steel surface. However, after surface chemical modification, the water jet could bounce off easily from the surface (**Fig. 7 c**). This is because lowered surface energy and the presence of air cushion formed by the trapped air between the solid and liquid [35] which do not allow the impacting water jet to enter in the rough structure of the surface. The water jet was targeted at the same position for around 1 min, then scanned over whole surface and water jet was still bouncing off the surface continuously, confirming no damage to the surface. A video of water jet striking on the superhydrophobic steel surface is shown in supporting information.

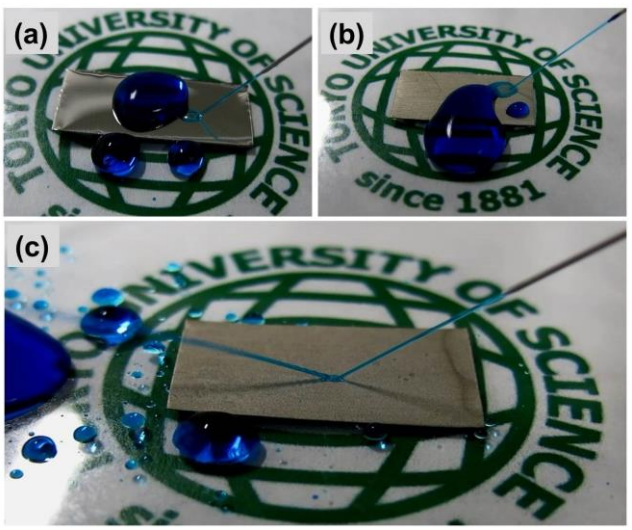

Figure 7. Optical photographs of water jet impact on (a) B-430-SS (b) E-430-SS/8h (c) M-430-SS/8h.

A sandpaper abrasion test was performed on the superhydrophobic steel surface as shown in **Fig. 8** (steps 1-5). After abrasion, water drops (~8 µl) placed on the steel surface acquired a contact angle of ~ 153° (step 4); however they remain

adhered on the surface after 90° and 180° of tilting (step 5). This explains that the non-sticky superhydrophobic nature of steel surface was irreversibly changed to sticky superhydrophobic nature. Further this abrasion tested surface is studied with FE-SEM and laser microscope techniques. As shown in the surface morphology images (**Fig S3)**, abundant and severe scratches were observed on the surface, which is mainly responsible for the permanent switch in the wetting properties. The laser microscopy analysis (**Fig. S4**) showed that the surface roughness found to decrease to ~1.18 µm after abrasion test. This corroborate that the surface roughness of superhydrophobic surface can be altered during strong abrasion.

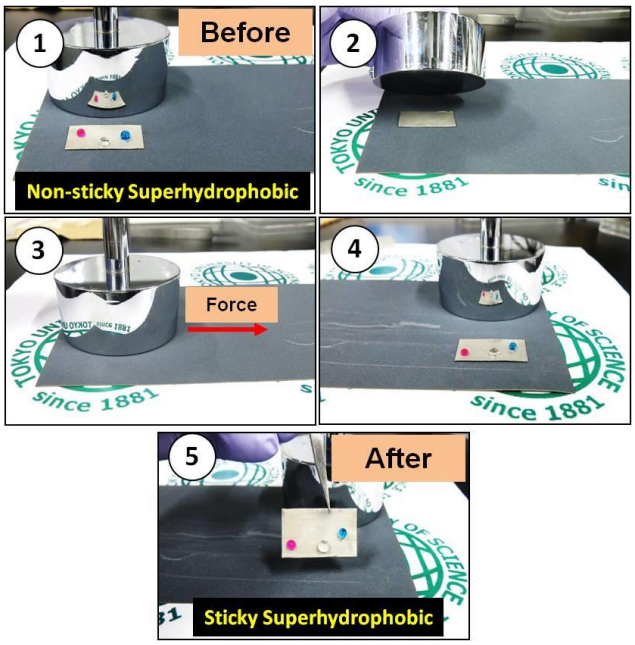

Figure 8. Sandpaper abrasion test on the superhydrophobic M-430-SS/8h surface.

A similar switching in wettability like after sandpaper abrasion test was observed in case of adhesive tape peeling test. The different stages of adhesive tape peeling test are presented in **Fig. 9.** Before applying adhesive tape, the steel surface shows superhydrophobic properties (step 1) and turn to sticky superhydrophobicity (WCA~156° and no water drop sliding for upside down tilting) after peeling off the adhesive tape from the surface (step 2 to 4). We examined the surface morphology of this surface (**Fig. S5).** From **Fig. S5**, it is clearly understands that the rough porous structure (before test) is partially destroyed after tape peeling lead to decreasing the surface roughness to ~ 1.80 µm (**Fig. S5**). These results were consistence with switchable wetting property of steel surface as is discussed in Figure 8. Recently, Wang et al [36] have demonstrated mechanically stable superhydrophobic steel surface which endured its surface microstructure against sandpaper abrasion test as well as 70 times adhesive tape peeling tests.

The stable wetting characteristics of superhydrophobic steel surface was analysed against UV irradiation test. The sample was kept under UV light as shown in the inset of **Fig. S6** and the water contact angles were measured for every day. The superhydrophobic steel surface showed sustainable static water contact angle within 1% deviation. In addition, it shows stable sliding angle even after 1 week of continuous UV irradiation.

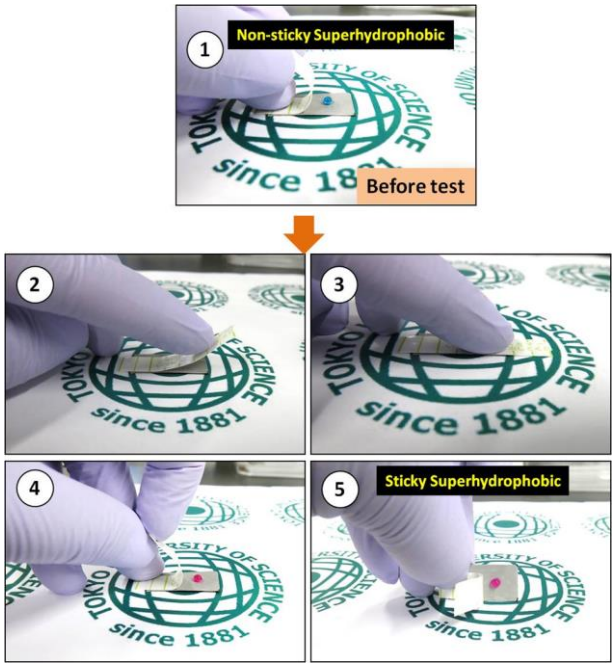

Figure 9. Adhesive tape peeling test on the superhydrophobic M-430-SS/8h surface.

Self-cleaning property of the coating

The surface which cleans themselves under the action of rolling water drops is known as superhydrophobic self-cleaning surface [37]. The air pockets trapped in between the rough structure can efficiently reduce the adhesion between water drops and the superhydrophobic surface and therefore any dust particles present on the surface can be easily picked by the rolling water drops. The self-cleaning ability of the superhydrophobic steel surface was studied. The Oil Red O powder was used as characteristic dust particles. We spread the dust particles on the superhydrophobic steel surface and water drop of volume 10 µl was rolled on the surface with the help of needle tip. The rolling water drop could easily pick up the dust particles from the surface keeping it clean and dust free. **Fig. 8a** shows the water drop enclosed by dust particles. A water drop collected almost all dust from the surface. This confirms the strong self-cleaning ability of the superhydrophobic steel surface. **Fig. 8b** shows the superhydrophobic steel surface floating on water surface. This steel substrate was constantly floating on water for more than 2 days, which confirms that the superhydrophobic surfaces strongly repels water and keep itself dry.

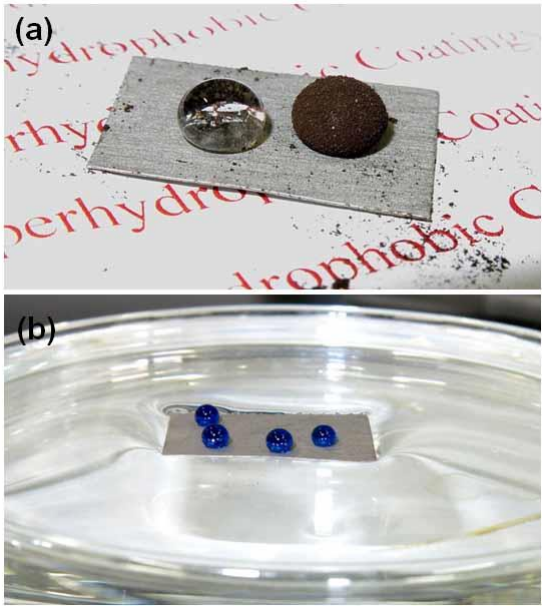

Figure 10. Optical photograph of self-cleaning behaviour of superhydrophobic M-430-SS/8h surface and (b) superhydrophobic M-430-SS/8h surface floating on water surface.

Corrosion resistance analysis

In order to explore the impact of the super hydrophobic surfaces on the corrosion resistance of the steel substrate, the potentiodynamic polarization curves of the B-430-SS, E-430-SS/8h and M-430-SS/8h surfaces in the 5 wt % NaCl aqueous solution are acquired from the electrochemical points of view and displayed in **Figure 11**. A closer assessment of the result implies that the corrosion potentials (E_{corr}) of both the E-430-SS/8h and M-430-SS/8h are shifted toward a more positive direction in comparison to the B-430-SS, signifying the appreciable protection for SS substrate through surface modification. Further, the corrosion current density (I_{corr}) of B-430-SS surface is found to be 4.70×10^{-3} A/cm^2 , whereas those of E-430-SS/8h and M-430-SS/8h surfaces are 3.13 $\times10^{-4}$ and 2.86×10^{-6} A/cm^2, respectively. In general, low current density confirms the improvement in corrosion protection performance of the superhydrophobic surface.[38] It is noteworthy to mention that the corrosion densities are decreased by more than 1 order for E-430-SS/8h surface and 3 orders for M-430-SS/8h surface compared to that of B-430-SS surface. Further, the value of the i_{corr} of the M-430-SS surface is much smaller, which designates that the corrosion resistance of M-430-SS/8h surface is higher than that of the E-430-SS/8h surface. The enhanced corrosion resistance for the M-430-SS/8h surface probably correlated to the fact that the superhydrophobic surfaces cannot be wetted underwater, and thus, harboured the SS surface against corrosion in NaCl solution.

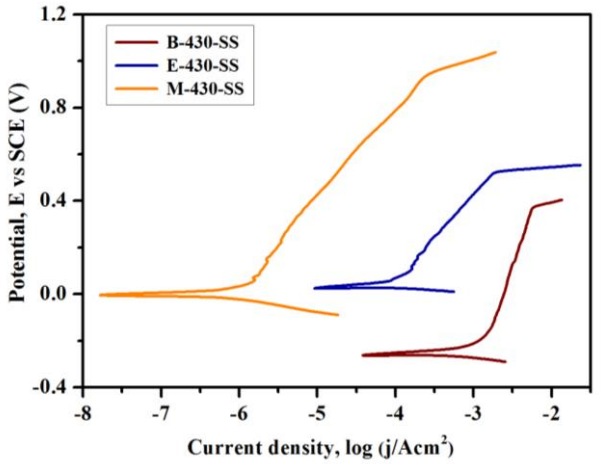

Figure 11. Potentiodynamic curves of B-430-SS, E-430-SS/8h and M-430-SS/8h surface after immersion in 5 wt % NaCl aqueous solution.

Figure 12 represents the Nyquist plots obtained for the B-430-SS, E-430-SS/8h and M-430-SS/8h surfaces in the 5 wt % NaCl aqueous solution. Nyquist plots exhibited large, incomplete semicircles, which indicate a capacitive behaviour[39]; the semicircle diameter have higher values for the M-430-SS/8h surface than those of the B-430-SS and E-430-SS/8h surface. In general, a higher semicircle diameter (charge transfer resistance) signifies a lower corrosion rate.[40] It can be seen that the M-430-SS/8h surface exhibited the highest impedance value around 5.0×10^{6} $\Omega\cdot$cm $^{-2}$ that is 3 orders higher than that of the B-430-SS surface (7.5×10^{3} $\Omega\cdot$cm $^{-2}$) and 2 orders higher than that of the E-430-SS/8h (1.8×10^{4} $\Omega\cdot$cm $^{-2}$). These results obviously reveal that the M-430-SS/8h surface protects the SS substrate against corrosion better than the E-430-SS/8h and B-430-SS. Hence, it could be concluded that the superhydrophobic surface acts as a physical barrier between the metal and environment, offering the improved corrosion resistance.

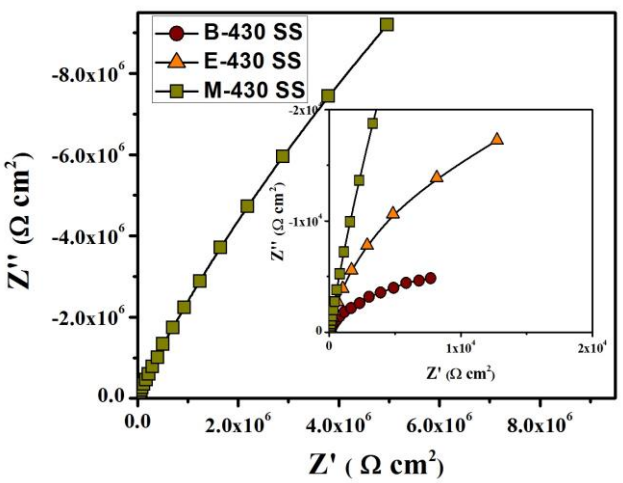

Figure 12. Nyquist plots of B-430-SS, E-430-SS/8h and M-430-SS/8h surface after immersion in 5 wt % NaCl aqueous solution (inset: enlarged impedance spectra).

Conclusions

The superhydrophobic steel surface was prepared by creating rough structure and subsequent lowering its surface energy. Water drops acquires spherical shape on this superhydrophobic steel surface with contact angle of 164±3º. As the water drop slide off the surface at sliding angle of 9±2º, the dust particles accumulated on the surface were washed out under the action of rolling water drops, confirming the self-cleaning behaviour. The stream of water jet eventually bounces off the surface without damaging the surface features hence maintaining the superhydrophobicity. The steel surface preserved its superhydrophobicity under low and harsh mechanical bending. Although, the superhydrophobic steel showed stable wetting property under harsh mechanical bending, the wettability is switching to sticky superhydrophobic after sandpaper abrasion test and adhesive tape peeling test. It is suggesting further research necessitate to sustain the wetting property under strong surface perturbation conditions. The steel surface preserved its excellent superhydrophobic wetting state under continuous UV light irradiation for more than 1 week. The enhanced corrosion resistance in the modified SS surface originated from the superhydrophobic surfaces prevent the possibility of the corrosion process and protect the substrates for long time. Such stable superhydrophobic metal surfaces can find potential industrial applications.

Acknowledgements

This research work is supported by the Japan Society for the Promotion of Science (JSPS), Postdoctoral Fellowship Program for Foreign Researchers, SSL (ID: P13067) and PS (ID:13374).

Notes and references

[a] *Photocatalysis International Research Center, Tokyo University of Science, 2641 Yamazaki, Noda, Chiba 278-8510, Japan. E-mail: fujishima_akira@admin.tus.ac.jp*
[b] *Center of Research Excellence in Corrosion, King Fahd University of Petroleum and Minerals, Dhahran 31261, Kingdom of Saudi Arabia.*
[c] *Institute of Environmental and Analytical Sciences, College of Chemistry and Chemical Engineering, Henan University, Kaifeng 475001, P.R. China.*
Electronic Supplementary Information (ESI) available: [details of EDS analysis is included]. See DOI: 10.1039/b000000x/

1. W. Barthlott and C. Neinhuis, *Planta*, 1997, **202**, 1-8.
2. D. Byun, J. Hong, Saputra, J. H. Ko, Y. J. Lee, H. C. Park, B.-K. Byun and J. R. Lukes, *Journal of Bionic Engineering*, 2009, **6**, 63-70.
3. X. Gao and L. Jiang, *Nature*, 2004, **432**, 36-36.
4. R. N. Wenzel, *Ind. Eng. Chem.*, 1936, **28**, 988-994.
5. A. Cassie, *Discussions of the Faraday Society*, 1948, **3**, 11-16.
6. S. S. Latthe and A. L. Demirel, *Polymer Chemistry*, 2013, **4**, 246-249.
7. H. Yabu and M. Shimomura, *Chem. Mater.*, 2005, **17**, 5231-5234.
8. L. Xu and J. He, *Langmuir*, 2012, **28**, 7512-7518.
9. S. S. Latthe, C. Terashima, K. Nakata, M. Sakai and A. Fujishima, *Journal of Materials Chemistry A*, 2014, **2**, 5548-5553.
10. S. De, D. Jana, S. K. Medda and G. De, *Industrial & Engineering Chemistry Research*, 2013, **52**, 7737-7745.
11. H. Yoon, S.-H. Na, J.-Y. Choi, S. S. Latthe, M. T. Swihart, S. S. Al-Deyab and S. S. Yoon, *Langmuir*, 2014, **30**, 11761-11769.
12. H. Ogihara, J. Xie, J. Okagaki and T. Saji, *Langmuir*, 2012, **28**, 4605-4608.
13. J. Li, L. Yan, Q. Ouyang, F. Zha, Z. Jing, X. Li and Z. Lei, *Chem. Eng. J.*, 2014, **246**, 238-243.
14. H. Zhou, H. Wang, H. Niu, A. Gestos, X. Wang and T. Lin, *Adv. Mater.*, 2012, **24**, 2409-2412.
15. X. Zhou, Z. Zhang, X. Xu, F. Guo, X. Zhu, X. Men and B. Ge, *ACS Applied Materials & Interfaces*, 2013, **5**, 7208-7214.
16. S. Wang, L. Feng and L. Jiang, *Adv. Mater.*, 2006, **18**, 767-770.
17. H. Wang, J. Yu, Y. Wu, W. Shao and X. Xu, *Journal of Materials Chemistry A*, 2014, **2**, 5010-5017.
18. X. Du, J. S. Li, L. X. Li and P. A. Levkin, *Journal of Materials Chemistry A*, 2013, **1**, 1026-1029.
19. S. Latthe, C. Terashima, K. Nakata and A. Fujishima, *Molecules*, 2014, **19**, 4256-4283.
20. L. Li, V. Breedveld and D. W. Hess, *ACS Applied Materials & Interfaces*, 2012, **4**, 4549-4556.
21. S. Yuan, S. O. Pehkonen, B. Liang, Y. P. Ting, K. G. Neoh and E. T. Kang, *Corros. Sci.*, 2011, **53**, 2738-2747.
22. Z. Chen, Y. Guo and S. Fang, *Surf. Interface Anal.*, 2010, **42**, 1-6.
23. B. Qian and Z. Shen, *Langmuir*, 2005, **21**, 9007-9009.
24. P. Li, X. Chen, G. Yang, L. Yu and P. Zhang, *Appl. Surf. Sci.*, 2014, **300**, 184-190.
25. L. Liu, F. Xu and L. Ma, *The Journal of Physical Chemistry C*, 2012, **116**, 18722-18727.
26. M. Toma, G. Loget and R. M. Corn, *ACS Applied Materials & Interfaces*, 2014, **6**, 11110-11117.
27. S. E. Lee, D. Lee, P. Lee, S. H. Ko, S. S. Lee and S. U. Hong, *Macromolecular Materials and Engineering*, 2013, **298**, 311-317.
28. T.-H. Kim, S.-H. Ha, N.-S. Jang, J. Kim, J. H. Kim, J.-K. Park, D.-W. Lee, J. Lee, S.-H. Kim and J.-M. Kim, *ACS Applied Materials & Interfaces*, 2015, **7**, 5289-5295.
29. H. S. Khoo and F.-G. Tseng, *Nanotechnology*, 2008, **19**, 345603.
30. J. Guo, S. Yu, J. Li and Z. Guo, *Chem. Commun.*, 2015, **51**, 6493-6495.
31. A. Kibar, H. Karabay, K. S. Yiğit, I. Ucar and H. Y. Erbil, *Exp. Fluids*, 2010, **49**, 1135-1145.
32. Y. C. Jung and B. Bhushan, *ACS Nano*, 2009, **3**, 4155-4163.
33. Z. Wang, C. Lopez, A. Hirsa and N. Koratkar, *Appl. Phys. Lett.*, 2007, **91**, 023105-023105-023103.
34. S. S. Latthe, P. Sudhagar, C. Ravidhas, A. Jennifer Christy, D. David Kirubakaran, R. Venkatesh, A. Devadoss, C. Terashima, K. Nakata and A. Fujishima, *CrystEngComm*, 2015, **17**, 2624-2628.
35. C. Luo, H. Zheng, L. Wang, H. Fang, J. Hu, C. Fan, Y. Cao and J. Wang, *Angew. Chem.*, 2010, **122**, 9331-9334.
36. N. Wang, D. Xiong, Y. Deng, Y. Shi and K. Wang, *ACS Applied Materials & Interfaces*, 2015, **7**, 6260-6272.
37. H. Yoon, H. Kim, S. S. Latthe, M.-w. Kim, S. Al-Deyab and S. S. Yoon, *Journal of Materials Chemistry A*, 2015.
38. Y. Cheng, S. Lu, W. Xu and H. Wen, *RSC Advances*, 2015, **5**, 15387-15394.
39. A. Madhankumar, S. Nagarajan, N. Rajendran and T. Nishimura, *J. Solid State Electrochem.*, 2012, **16**, 2085-2093.
40. A. Madhan Kumar, R. Suresh Babu, I. B. Obot and Z. M. Gasem, *RSC Advances*, 2015, **5**, 19264-19272.

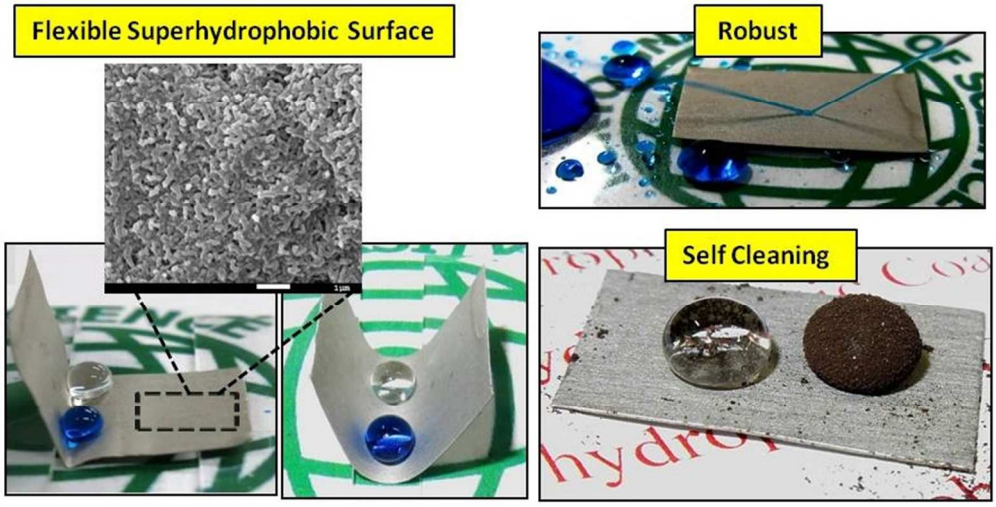

150x76mm (150 x 150 DPI)